Soft Matter

Translucent in air and iridescent in water: structural analysis of a salamander egg sac

SUPPLEMENTARY FILE

Aleksandra V. Zabuga[1], Marcelle I. Arrigo[1], Jérémie Teyssier[2],
Sébastien R. Mouchet[3,4], Kanto Nishikawa[5], Masafumi Matsui[5],
Miguel Vences[6], and Michel C. Milinkovitch[1*]

1. Laboratory of Artificial and Natural Evolution (LANE), Department of Genetics and Evolution, University of Geneva, Switzerland.
2. Department of Quantum Matter Physics, University of Geneva, Switzerland.
3. School of Physics, University of Exeter, Exeter EX4 4QL, UK.
4. Department of Physics, University of Namur, 5000 Namur, Belgium.
5. Graduate School of Human and Environmental Studies, Kyoto University, Kyoto, Japan.
6. Zoological Institute, Braunschweig University of Technology, Braunschweig, Germany.

*Correspondence to: Michel C. Milinkovitch,
Laboratory of Artificial & Natural Evolution (LANE),
Dept. of Genetics & Evolution, University of Geneva,
Sciences III, 30, Quai Ernest-Ansermet, 1211 Geneva 4, Switzerland.
Tel: +41(0)22 379 67 85; e-mail: Michel.Milinkovitch@unige.ch

Supplementary Note 1: Surface diffraction grating model.

The striations that form the surface grating of Fig. 1f are the inner boundary of a slanted (almost to 90°) volume phase holographic grating[1-4] composed from the fibres observed in figure 2d and figure 3. Here, we show that the *Hynobius* egg sac optical response (Fig. 4 and Fig. S1) can be quantitatively explained by a simple model of a surface diffraction grating. The figure S2a schematically illustrates the path that light travels in a backscattered geometry. The egg sac envelope has an average refractive index n_2=1.38, *i.e.*, larger than that of water (n_1=1.33). The backscattered wavelength is derived from the grating equation:

$$\lambda = d \cdot n_2 \cdot 2 \cdot \sin\theta_3 \qquad \text{Eq. 1}$$

where n_2 is the refractive index of the egg sac's material, λ is the light wavelength, and d is the diffraction grating period. Considering that the thickness of the egg envelop is small compared to the egg radius, we can reasonably assume that $\theta_3 \sim \theta_2$. Using Snell's law at the interface between the external medium and the egg envelope

$$n_1 \cdot \sin\theta_1 = n_2 \cdot \sin\theta_2 = n_2 \cdot \sin\theta_3 \qquad \text{Eq. 2}$$

equation 1 becomes:

$$\lambda = d \cdot n_1 \cdot 2 \cdot \sin\theta_1 \qquad \text{Eq. 3}$$

where n_1 is the refractive index of water or air (depending if the egg sac is submerged or removed out of the water, respectively).

We can now compute the colour distribution along the egg sac's circumference (Fig. S2b). In the optical experiments (Fig. 4), the incident light angle relative to the egg sac surface (θ_1) changes along the egg sac curvature from nearly 0° at the centre towards grazing incidence at the edges. Equation 3 can be modified such that sin θ_1 is substituted with x/R (where *x* is the distance from the centre of the sac to the outer or the inner edge, and *R* is the egg sac's radius) to give:

$$\lambda = 2 \cdot d \cdot n_1 \cdot \frac{x}{R} \qquad \text{Eq. 4}$$

The egg sac's radius is 1 cm, so the value of *x* varies from 0 cm to 1 cm or -1cm when moving from the centre towards the outer or inner edge, respectively (Fig. S2b). In water, the outer curvature of the egg sac (x=-1) is mostly green-blue (Fig. 4a), and matches with the colour distribution computed with equation 4 when the diffraction grating period is 190 nm (Fig. S2b), while the colours on the inner curvature span a larger range of wavelengths from yellow to blue (Fig. 4c) and correspond to a larger diffraction grating period of 230 nm. The model (Fig. S2b) also predicts that removing the egg sac from water causes a blue shift resulting in the loss of essentially all colours in the visible range at the outer curvature, whereas some blue iridescence is maintained at the very edge of the inner curvature. These results match the experimental data (Fig. 4).

The different diffraction grating periods at the outer and inner curvature of the egg sac could result from the former being more stretched than the latter because of the crescent shape of the sac: the fibres at the outer curvature might become thinner and closer packed due to the stretch along the Z-axis while, at the inner curvature, they would become thicker and more distant because of compression along the Z-axis.

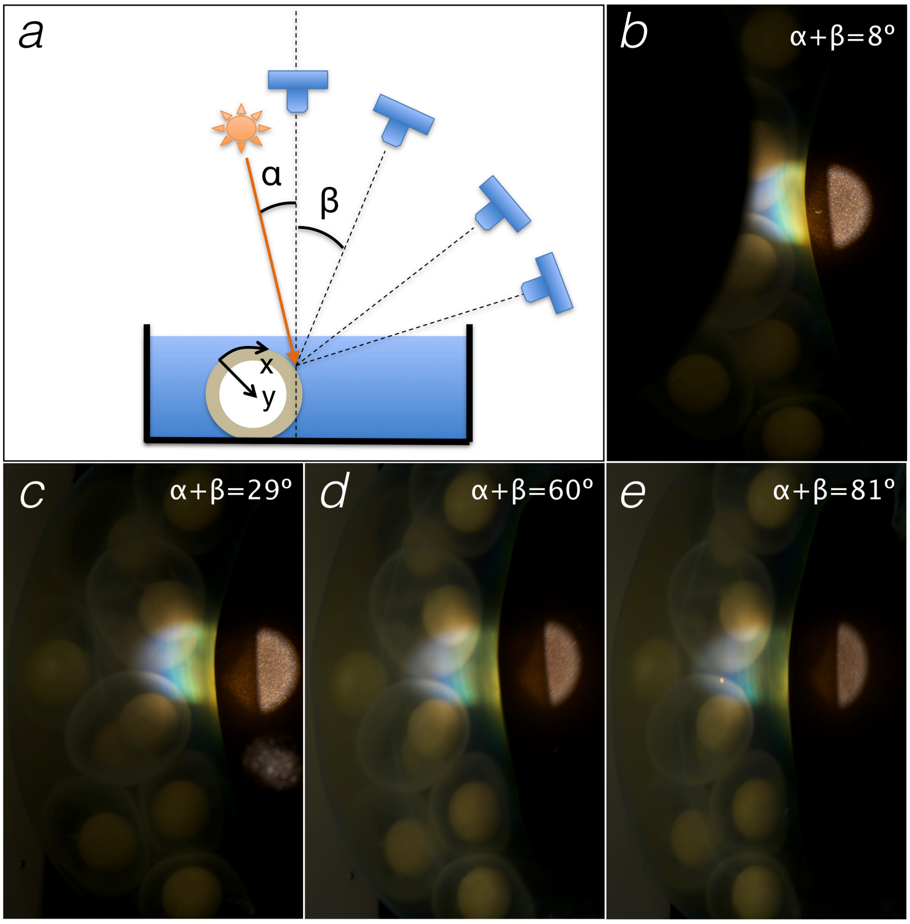

Supplementary Figure S1. The iridescence of the egg sac in water at different angles of observation β. The incident light angle (α=8°) is fixed.

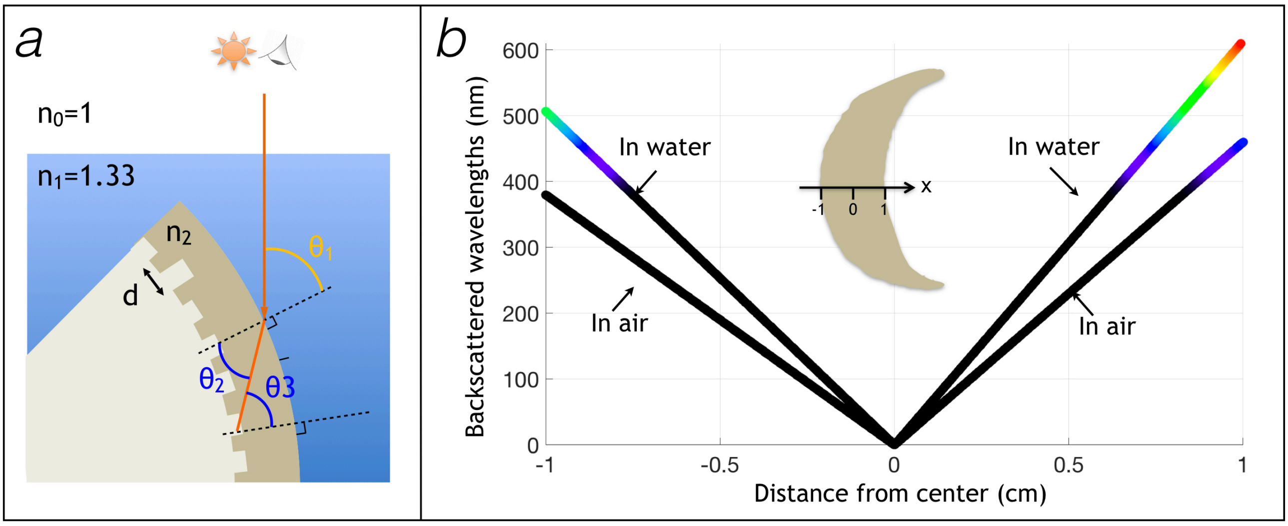

Supplementary Figure S2. (**a**) Schematic representation of the backscattered optical path of the light diffracted from the egg sac's material when the surface of the water is hit with an approximately perpendicular incident angle; n_0, n_1, n_2 are refractive indices of the corresponding media/materials, *d* is the diffraction grating period; θ_1 to θ_3 are incidence and refraction angles. (**b**) Colour distribution along the egg sac's circumference computed using this simplified diffraction grating model; grating period = 190 nm and 230 nm for the outer and inner curvatures, respectively.

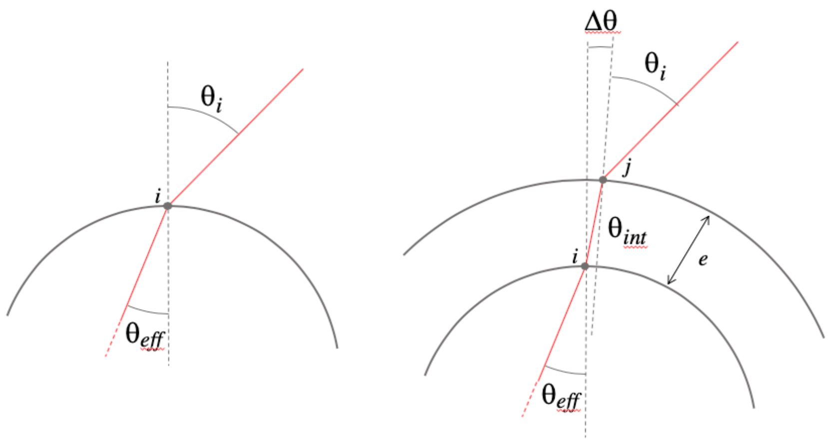

Supplementary Figure S3. Effective refractive angle θ_{eff} is not affected by the presence of a uniform thin layer of water on the egg. As *e* is small compared to the radius of the egg, Δθ is negligible and neither the refracted angle nor the spectral shift is affected by the presence of a layer of water at the envelope as long as this layer is thin and follows the shape of the sac.

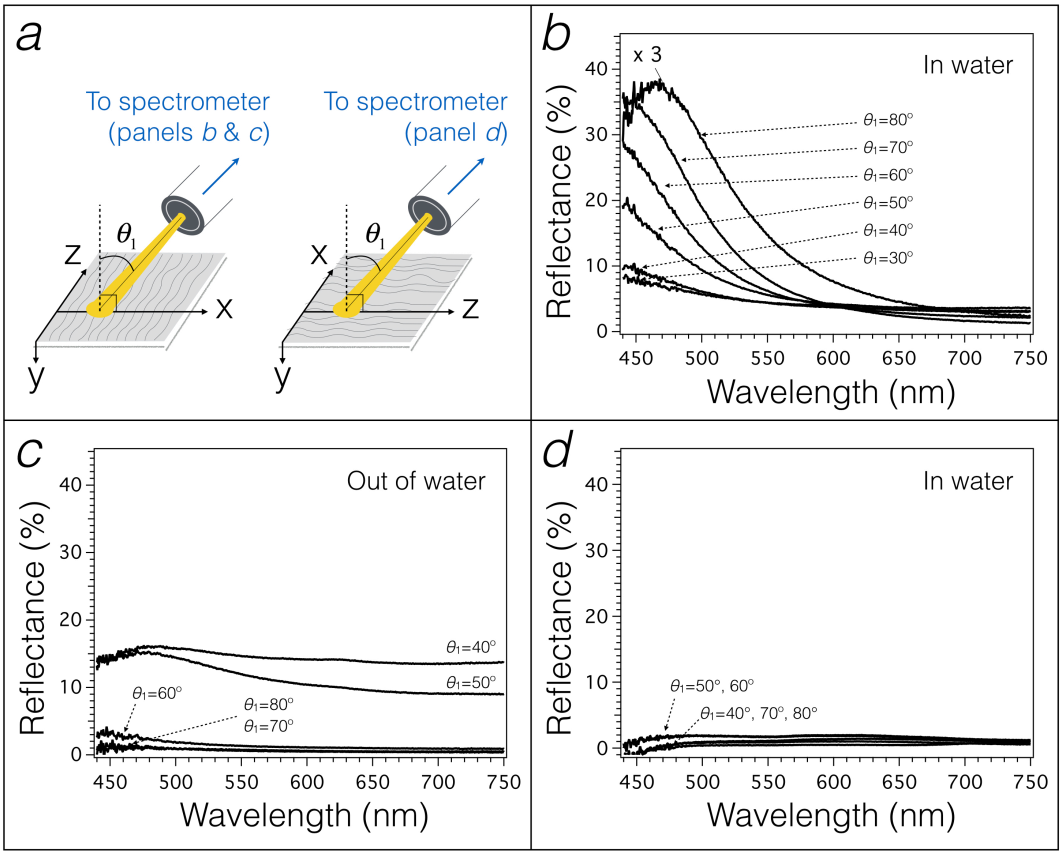

Supplementary Figure S4. (**a**-left panel, **b**, **c**) Backscattered spectra of the egg sac envelope under different incident light angles θ_1 with the X-axis in water (b) and in air (c). (**a**-right panel, **d**) Backscattered spectra of the egg sac envelope under different incident light angles θ_1 with the Z-axis in water. All spectra were smoothed with a spline function (spline parameter = 0.98) in Matlab.

Supplementary references

1. Kogelnik, H. Coupled wave theory for thick hologram gratings, *The Bell System Technical Journal* **1969**, *48*, 2909-2947.

2. Barden, S. C.; Arns, J. A.; Colburn, W. S. In Volume-phase holographic gratings and their potential for astronomical applications, *Astronomical Telescopes and Instrumentation*, SPIE: **1998**; p 11.

3. Brotherton-Ratcliffe, D. A treatment of the general volume holographic grating as an array of parallel stacked mirrors. *Journal of Modern Optics* **2012**, *59*, 1113-1132.

4. Loicq, J.; Venancio, L. M.; Stockman, Y.; Georges, M. P. Performances of volume phase holographic grating for space applications: study of the radiation effect. *Appl. Opt.* **2013**, *52*, 8338-8346.